Research Inventy: International Journal of Engineering And Science
Vol.14, Issue 11 (November 2024), PP 01-12
Issn (e): 2278-4721, Issn (p):2319-6483, www.researchinventy.com

Photooxidation of Roxithromycin and Erythromycin from Antibiotic-Containing Wastewater Using CeO_2 /ZnO Nanocomposite

AKÇAĞLAR Sevil
Department of Mechanical Engineering, Faculty of Engineering, Dokuz Eylül University, İzmir, Turkey, Corresponding Author: sevil.akcaglar@deu.edu.tr

Abstract: *This study investigates the photooxidation of Roxithromycin and Erythromycin, two prevalent antibiotics found in antibiotic industry wastewater, utilizing a CeO_2 /ZnO nanocomposite as a photocatalyst. The synthesized CeO_2 /ZnO nanocomposite exhibits enhanced photocatalytic activity under sun light irradiation, promoting the degradation of these antibiotics. Various parameters, including catalyst loading, initial antibiotic concentration, and reaction time, were systematically optimized to assess their influence on the photocatalytic efficiency. The results indicate significant degradation rates for both antibiotics. These findings underscore the potential of CeO_2 /ZnO nanocomposites as a viable solution for the remediation of antibiotic-contaminated wastewater, contributing to environmental sustainability and public health protection.*
Keywords: *cerium oxide, zinc oxide, photocatalytic degradation, antibacterial activity*

Date of Submission: 02-11-2024 Date of acceptance: 13-11-2024

I. INTRODUCTION

The proliferation of antibiotic-resistant bacteria represents a critical challenge in contemporary medicine, necessitating innovative approaches to mitigate the dissemination of pharmaceutical contaminants in the environment. Among these, macrolide antibiotics such as erythromycin and roxithromycin have garnered significant attention due to their widespread use in both human and veterinary medicine. Their presence in wastewater, resulting from pharmaceutical manufacturing, hospital effluents, and inadequate wastewater treatment processes, poses substantial risks to aquatic ecosystems and public health [1-2].

Chemotherapeutic agents, particularly antibiotics, play a pivotal role in both human and veterinary medicine for the prevention and treatment of microbial infections [3]. However, the environmental implications of their widespread use have garnered significant attention. Antibiotics are introduced into the environment from a multitude of sources, including household wastewater systems, hospital effluents, agricultural runoff, pharmaceutical manufacturing processes, livestock waste, and the improper disposal of unused or expired medications [4]. Consequently, these compounds have been consistently detected in aquatic environments at concentrations that can reach up to 1.3 µg/L [5-6].

The extensive usage contributes to the prevalence and persistence of antibiotics in aqueous environments, raising significant ecological concerns due to their biological activity and potential to induce antibiotic resistance in microbial populations [7-8]. The phenomenon of antibiotic resistance is increasingly recognized as a major public health challenge, exacerbated by the presence of resistant bacteria in wastewater, environmental waters, marine sediments, and aquatic organisms such as fish [9-10].

The ecological impact of antibiotic contamination is profound, as sub-inhibitory concentrations can promote the survival and proliferation of resistant strains, leading to the horizontal transfer of resistance genes among microbial communities [11]. This scenario not only threatens public health but also disrupts the balance of aquatic ecosystems, potentially leading to reduced biodiversity and altered ecological functions [12]. Recent studies have illustrated that the persistence of antibiotics in environmental matrices can select for resistant microorganisms, compounding the challenges faced in both clinical and environmental settings [13].

As such, addressing the issue of antibiotic contamination requires a multifaceted approach, including enhanced wastewater treatment technologies and public awareness regarding the proper disposal of pharmaceutical products. Understanding the pathways and impacts of antibiotic release into the environment is crucial for developing effective strategies to mitigate their adverse effects and to curb the rising tide of antibiotic resistance.The persistence of antibiotics in aquatic environments has garnered attention due to their potential to induce antimicrobial resistance (AMR) and disrupt ecological balance [14]. Roxithromycin and erythromycin, macrolide antibiotics, are particularly challenging to degrade due to their stable chemical structures [15]. Traditional wastewater treatment methods often fall short in eliminating these contaminants, highlighting the

need for advanced oxidation processes (AOPs) that leverage photocatalysis [16].Once in the aquatic environment, the MLs undergo biodegradation and non-biologically driven reactions such as photodegradation, adsorption and others. Photodegradation has been shown to be one of the most important transformation ways of MLs [17]. Generally, the photodegradation of MLs can proceed via direct and indirect photolysis. As MLs can barely absorb the solar light due to the lack of chromophoric groups in the saturated aliphatic ring systems, the rate of the direct photolysis of MLs can be predicted to be low. In comparison, the indirect photolysis of MLs mediated by photosensitizers, in most cases dissolved organic matter (DOM) plays an important role in the elimination of MLs. DOM is ubiquitous presented in aquatic environment. Upon light absorption, DOM can produce a series of reactive intermediates (RIs), including hydroxyl radicals (OH), singlet oxygen ($^1O_2$) and triplet DOM (^{3}DOM*) [18-20]. However, in some cases, DOM can also inhibit the photolysis of some antibiotics due to the light screening effect. The degradation products of antibiotics formed during the photodegradation process could show increased or decreased toxicity [21].

Erythromycin, a natural macrolide antibiotic, has been extensively utilized for its efficacy against a variety of bacterial infections. Conversely, roxithromycin, a semi-synthetic derivative of erythromycin, offers improved pharmacokinetic properties, leading to its increased application in clinical settings [22]. Both antibiotics exhibit low biodegradability and can persist in wastewater treatment plants, where they may undergo partial removal, resulting in sub-lethal concentrations that contribute to the development of antibiotic resistance in microbial populations.

Roxithromycin (ROX) is a widely used macrolide antibiotic and its environmental fate and ecotoxicity have attracted considerable attention Roxithromycin is a semi-synthethic macrolide antibiotic that is structurally and pharmacologically similar to erythromycin, azithromycin, or clarithromycin. It was shown to be more effective against certain Gram-negative bacteria, particularly *Legionella pneumophila*. Roxithromycin exerts its antibacterial action by binding to the bacterial ribosome and interfering with bacterial protein synthesis. It is marketed in Australia as a treatment for respiratory tract, urinary and soft tissue infections [23-24].

The removal of these contaminants from wastewater has therefore become a pressing issue. Conventional treatment methods, such as activated sludge processes and advanced oxidation techniques, often fall short in effectively degrading these compounds [25]. As a response, the application of nanotechnology in wastewater treatment has gained traction, particularly the use of metal oxide nanocomposites, which have demonstrated enhanced photocatalytic activity and adsorption capabilities [26].

Among various nanocomposites, cerium dioxide (CeO_2) and zinc oxide (ZnO) have emerged as promising candidates due to their unique physicochemical properties. CeO_2 is known for its high oxygen storage capacity and redox cycling ability, while ZnO exhibits excellent photocatalytic properties under UV light irradiation [27]. The combination of these two materials into a CeO_2 /ZnO nanocomposite may provide synergistic effects, enhancing the degradation and removal efficiency of antibiotic pollutants such as roxithromycin and erythromycin from contaminated water sources [28].

This study aims to investigate the efficacy of the CeO_2 /ZnO nanocomposite in the removal of roxithromycin and erythromycin from antibiotic-containing wastewater. By examining the photodegradation kinetics and optimal conditions (CeO_2 /ZnO nanocomposite concentration, Roxithromycin and Erythromycin concentrations time and pH) for maximum photodegradation yields of the aforementioned antibiotics, this research endeavors to contribute to the development of effective wastewater treatment strategies that can mitigate the environmental impact of antibiotic contaminants and help combat antibiotic resistance.

II. MATERIALS AND METHODS

2. Experimental Section

2.1. Chemicals

The analytical-grade chemicals utilized in this study included cerium nitrate (Ce $(NO_3)_3$) and zinc nitrate (Zn$(NO_3)_2$), both sourced from Merck India Pvt. Ltd. These chemicals were employed without further purification, ensuring their suitability for the intended experimental applications.Standards of roxithromycin and erythromycin, were procured from Sigma-Aldrich (St. Louis, MO, USA). Standard stock solutions at a concentration of 100 µg/mL for all compounds were prepared in methanol and stored in a dark environment at temperatures below 4 °C to prevent deterioration Extreme pure water (H_2 O) and methanol (CH_3 OH) of optimal grade were acquired from Fisher Scientific (Fair Lawn, NJ). Additionally, Whatman GFF glass fiber filters were employed for filtration processes.

2.2. Sample collection

The samples were collected from a antibiotic industry raw wastewater and maintained at +4 ^{o}C in a refrigerator until used in the photocatalytic analysis.

2.3. Antibiotic measurements

The concentrations of roxithromycin and erythromycin from an antibiotic-containing wastewater was analyzed using high performance liquid chromatography (HPLC) coupled with mass spectrometry (MS), HPLC worked with an Agilent C18 column (100 mm × 2.1 mm, 2.7 μm). Mobile phase A consisted of an equal volume mixture of methanol and acetonitrile, mobile phase B was formulated with 0.01 M CH_3COONH_4 and 0.05 % CH_3COOH, the mobile phase ratio of A: B = 60 %: 40 % (v/v), the flow velocity of mixed mobile phase was set at 0.2 mL/min, the sample volume extracted by the sampling needle was 5 ml.

2.4. Photodegradation Experiments

The photodegradation experiments were conducted to evaluate the efficiency of the CeO_2 /ZnO nanocomposite in facilitating the degradation of Roxithromycin and Erythromycin from antibiotic-containing wastewater. The experiments were performed in a batch reactor under controlled laboratory conditions.The concentrations of Roxithromycin and Erythromycin varied between 50 and 500 mg/l in the raw wastewater. Samples were withdrawn at regular intervals (10, 20, 30, 40 minutes) to monitor the photodegradation progress. The degradation efficiency was calculated using the formula:

Degradation Efficiency (%) = $\frac{C_0 - Ct}{C_0}$ x 100

where C_0 is the initial concentration of the antibiotic and Ct is the concentration at time t.
Additionally, control experiments without the nanocomposite and under dark conditions were conducted to isolate the effects of light and the CeO_2 /Zn catalyst concentrations on the photodegradation yields. The influence of various parameters, such as pH, initial antibiotic concentration, and catalyst loading, on the photodegradation rates was also systematically investigated. O nanocomposites in wastewater treatment applications.

2.2. Sample Characterization

The characterization of the CeO_2 /ZnO nanocomposite was conducted using a variety of analytical techniques to elucidate its structural, morphological, and optical properties, which are critical for understanding its photocatalytic activity in the degradation of antibiotics.

X-ray Diffraction (XRD) analysis was performed to determine the crystalline phases and purity of the synthesized nanocomposite. The XRD patterns were recorded over a range of 20° to 80° (2θ) using a diffractometer (Bruker D8) with Cu Kα radiation. The presence of distinct peaks corresponding to CeO_2 and ZnO confirmed the successful synthesis of the nanocomposite, and the average crystallite size was calculated using the Scherrer equation.

Scanning Electron Microscopy (SEM) was utilized to investigate the surface morphology and particle size of the CeO_2 /ZnO nanocomposite. Samples were coated with a thin layer of gold to enhance conductivity during imaging. SEM micrographs revealed a homogeneous distribution of nanoparticles and provided insights into the particle agglomeration behavior, which is critical for assessing their photocatalytic performance.

Transmission Electron Microscopy (TEM) was employed to further analyze the internal structure and morphology at the nanoscale. The TEM images facilitated the measurement of particle size distribution, revealing that the majority of particles were within the range of 10 to 30 nm, which is favorable for enhanced photocatalytic activity.

Fourier Transform Infrared Spectroscopy (FTIR) was conducted to investigate the functional groups present in the CeO_2 /ZnO nanocomposite. The FTIR spectra displayed characteristic absorption bands associated with metal-oxygen bonds, indicating successful incorporation of both CeO_2 and ZnO. The presence of hydroxyl groups was also noted which are known to participate in photocatalytic reactions.

UV-Vis Diffuse Reflectance Spectroscopy (DRS) was performed to evaluate the optical properties of the nanocomposite. The band gap energy was calculated from the DRS data using the Kubelka-Munk function, revealing a narrowed band gap compared to pure ZnO, which is advantageous for extending light absorption into the visible spectrum and enhancing photocatalytic efficiency.

The UV-Vis absorption spectra of the samples were recorded in the wavelength range of 200 to 800 nm using a spectrophotometer (Agilent Technologies, Cary 60). The absorbance data were utilized to calculate the band gap energy (Eg) using the Tauc equation:

$(\alpha h V)^n = A (h V - Eg)$

where α\alphaα is the absorption coefficient, h is Planck's constant, ν\nuν is the frequency of the incident light, Ais a constant, and n is a value that depends on the nature of the transition (1/2 for direct transitions) (Tauc, 1970).

The Debye-Scherrer formula used to determine the particle size is as follows.

$$D = 0.9 \lambda / \beta \cos \Theta \quad (1)$$

Where D is the crystallite size, λ is the wavelength of X-ray radiation (1.5418 Å), β is the full-width half maximum of the diffraction peak and Θ is the scattering angle.

III. RESULTS AND DISCUSSION

3.1. Characterization of the CeO_2 /ZnO Photocatalysts

The X-ray diffraction (XRD) spectra of ZnO, CeO_2 , and synthesized CeO_2 /ZnO composites, are decipted in Figure 1. The spectra exhibit several peaks that can be indexed based on diffraction patterns of ZnO (JCPDS card no. 36-1451) and CeO_2 (JCPDS card no. 34-0394). For CeO_2 /ZnO photocatalysts , the peaks observed at 2θ angles of 32.87°, 35.51°, 37.32°, 48.61°, 56.67°, 63.96°, 69.08°, and 69.99° correspond to the crystallographic planes (101), (003), (102), (103), (102), (105), (113), and (214), confirming the hexagonal wurtzite structure characteristic of ZnO .The peaks consistent with the polycrystalline structures of the individual oxides, suggesting the successful formation of CeO_2 /ZnO nanocomposite materials without the presence of secondary phases or impurities [29].

Figure 1. X-ray diffraction (XRD) spectra of ZnO, CeO_2 , and synthesized CeO_2 /ZnO composites

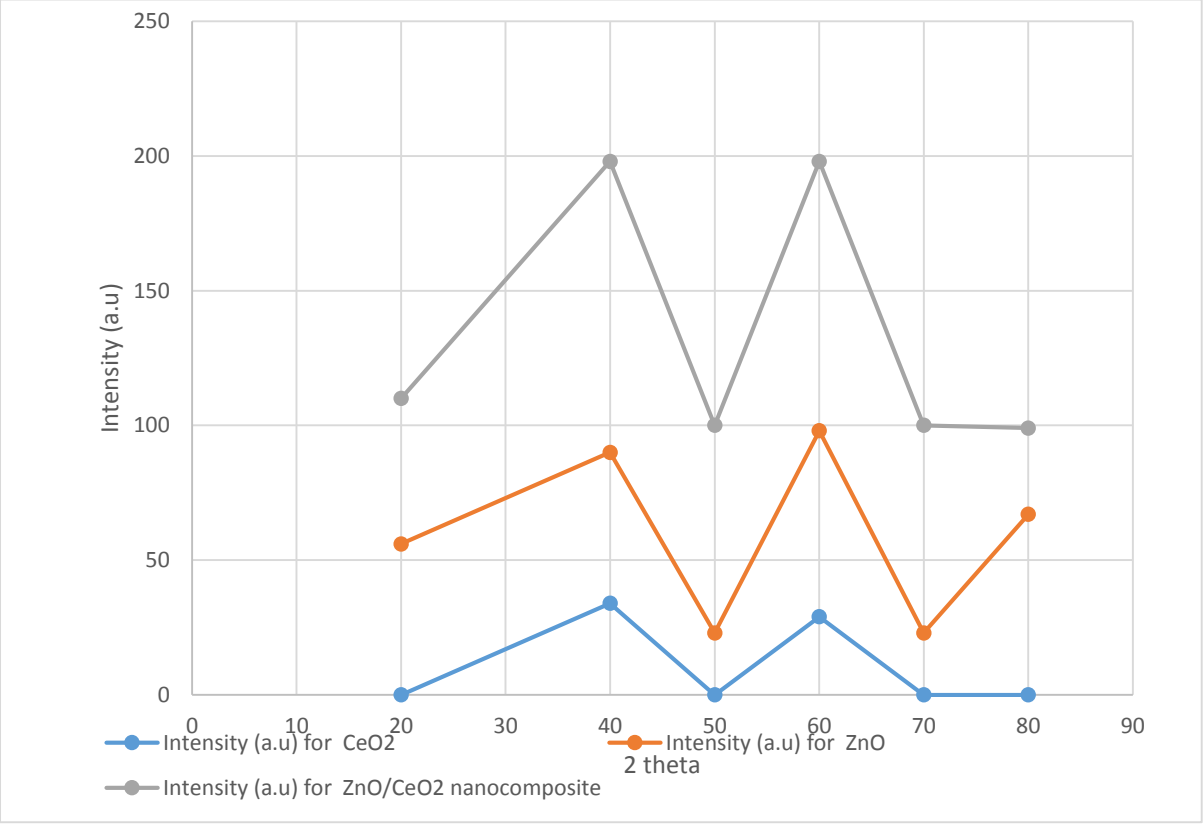

3.2. FTIR Analysis of the CeO_2 /ZnO Photocatalysts

The crystallite size varies from below 0.1 µ to approximately 3 µ. The accumulation of micro-crystallites was detected. The crystallites try to reach the minimum energy state, minimizing the contact area with the external environment. The small size of the obtained crystallites explains the good photocatalytic activity. The FTIR spectra are presented in Figure 2. FTIR analysis confirms that the organic phase has been eliminated by calcination. The peaks in the 3400–3450 cm^{-1} range are due to adsorbed water molecules (the O-H bond stretching vibration), and those in the 550–400 cm^{-1} range are generated by the vibrations of the metal oxide bonds [30].

Figure 2. FT-IR spectra of ZnO, CeO_2 , and synthesized CeO_2 /ZnO composites

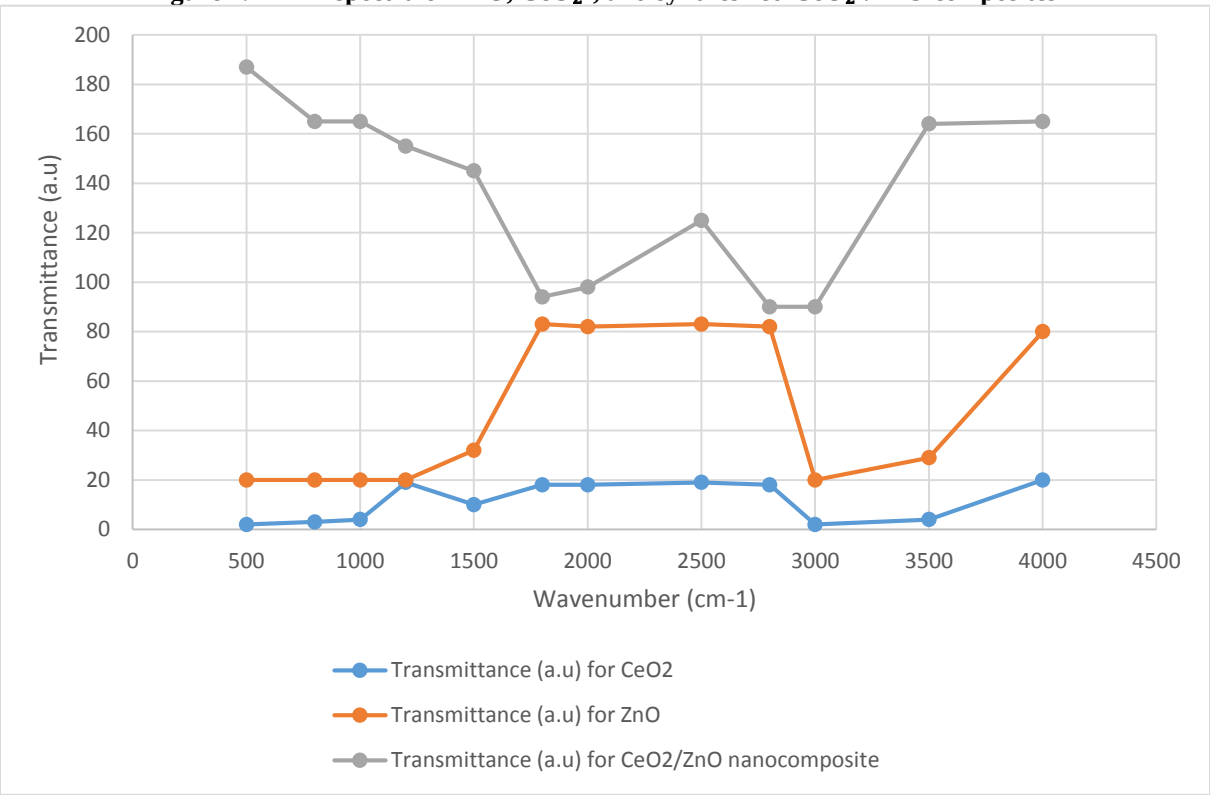

3.3 UV-Vis Spectroscopy analysis of CeO_2 /ZnO Photocatalysts

Ultraviolet-visible (UV-Vis) spectroscopy was employed to investigate the optical properties of the synthesized ZnO/CeO_2 nanocomposites. The UV-Vis spectra exhibited distinct absorption peaks indicating the successful incorporation of both ZnO and CeO_2 . The results demonstrated a significant shift in the absorption edge towards longer wavelengths compared to pure ZnO, suggesting a reduction in the band gap energy due to the formation of the composit [31-33]. The band gap energy of the ZnO component was found to be approximately 3.2 eV, while the nanocomposites exhibited band gap energies ranging from 2.8 to 3.0 eV, depending on the composition and synthesis conditions (Figure 4). These findings highlight the potential of ZnO/CeO_2 nanocomposites for enhanced photocatalytic activity under visible light irradiation.

Figure 4. UV-VIS spectra of ZnO, CeO_2 , and synthesized CeO_2 /ZnO composites

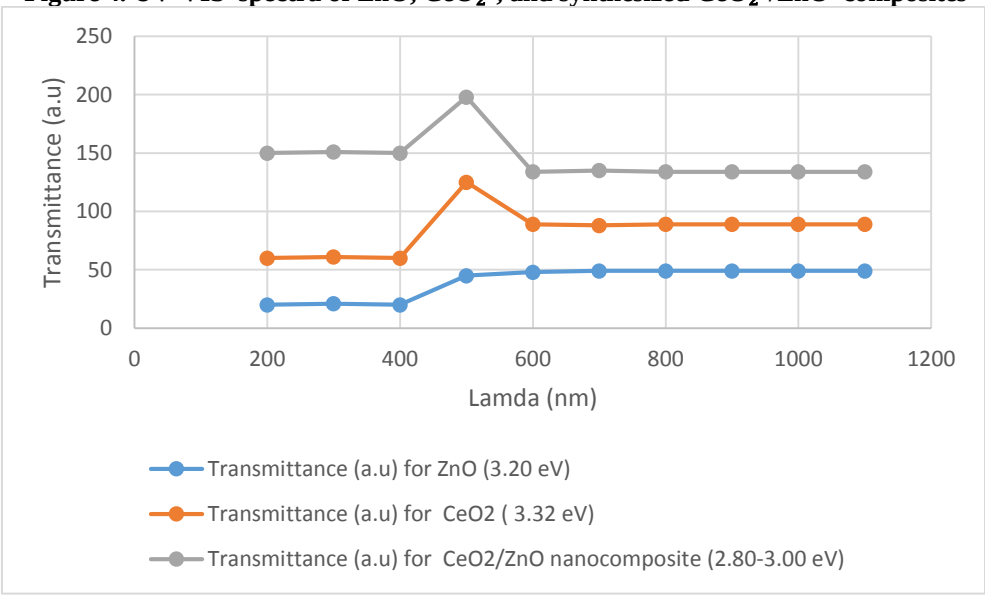

3.5. Photoluminescence Analysis of CeO_2 /ZnO Photocatalysts

Figure 5 presents the photoluminescence (PL) spectrum of the CeO_2 -ZnO nanocomposite. The primary objective of this PL study was to elucidate the presence of structural deficiencies within the crystal lattices of the nanomaterials. Typically, zinc oxide nanoparticles (ZnO NPs) characterized by numerous crystalline defects exhibit PL bands in the visible spectral region, which are indicative of such defects.In the analyzed spectrum, a prominent blue emission peak was observed at approximately 479 nm, attributed to the intrinsic luminescence of the CeO_2 component. Additionally, a series of peaks ranging from 479 to 575 nm can be observed, which result from the interaction and mixing of the luminescence from both CeO_2 and ZnO [35]. Notably, an orange emission peak at 594 nm was also recorded, which further signifies the presence of specific defect states within the nanocomposite structure [36].These luminescent characteristics highlight the potential of the CeO_2 -ZnO nanocomposite for applications in optoelectronics and photocatalysis, where the emission properties can be exploited to enhance performance [37].

Figure 5. Photoluminescence Analysis of CeO_2 /ZnO Photocatalysts

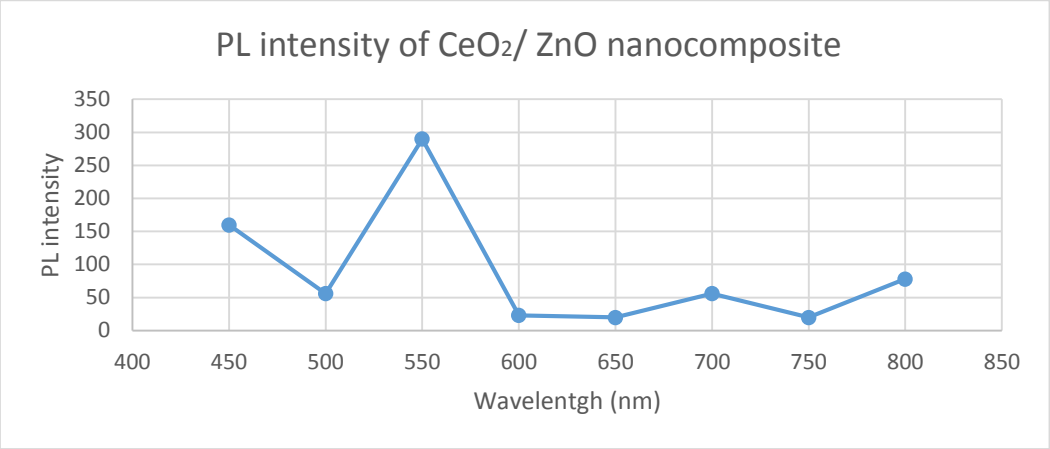

3.6. SEM Analysis of CeO_2 /ZnO Photocatalysts

The morphology of the synthesized CeO_2 -ZnO nanocomposite was examined using scanning electron microscopy (SEM), as illustrated in Figures 6a and 6b. The SEM images reveal a spongy, cave-like morphology, indicative of a highly porous structure. This unique morphology is beneficial, as it significantly enhances the surface area of the material, thereby facilitating improved catalytic activity [38]. The porosity of the CeO_2 -ZnO nanocomposite is critical for its performance in photocatalytic applications, as it increases the accessibility of reactants to active sites, leading to enhanced interaction and subsequent degradation of contaminants [39].

Figure 6. (a), (b) SEM images of CeO_2 /ZnO Photocatalysts

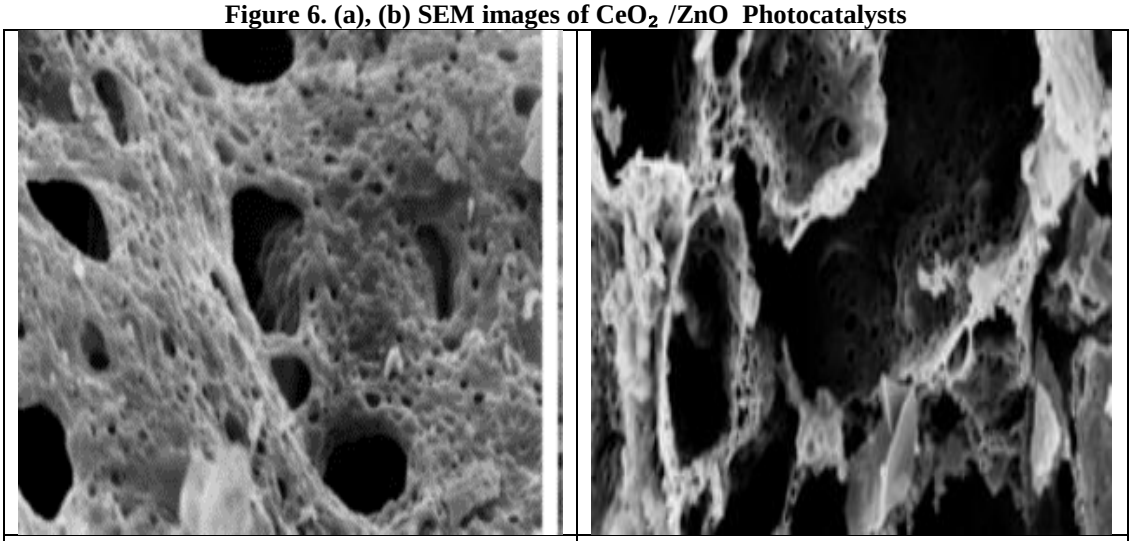

(a) 1µm | (b) 2µm

3.7. TEM Analysis of CeO_2 /ZnO Photocatalysts

Transmission electron microscopy (TEM) was utilized to elucidate the morphological and structural characteristics of the synthesized CeO_2 /ZnO nanocomposite, which is critical for understanding its photocatalytic properties in the degradation of pharmaceutical contaminants such as Roxithromycin and Erythromycin. The TEM images, presented in Figures 7a and 7b, reveal a well-dispersed arrangement of nanoparticles with predominantly spherical shapes and an average diameter ranging from 10 to 30 nm. This nanoscale dimension is advantageous for enhancing the photocatalytic surface area, thereby facilitating improved degradation efficiency [40]. The detailed morphological insights provided by TEM analysis support the hypothesis that the structural characteristics of the CeO_2 /ZnO nanocomposite play a significant role in its efficacy as a photocatalyst for the removal of antibiotic pollutants from wastewater. The uniform distribution and small particle size are likely to contribute to enhanced light absorption and increased active sites for the photocatalytic reactions [41].

Figure 7. (a), (b) TEM analysis results of CeO_2 /ZnO Photocatalysts

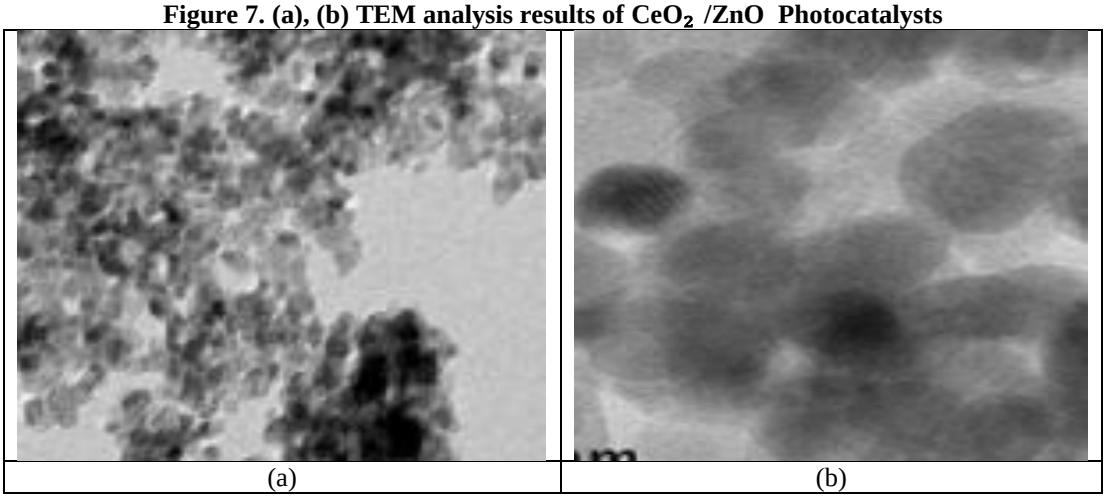

(a) (b)

The selected area electron diffraction (SAED) patterns obtained from the TEM analysis further confirmed the crystalline nature of the nanocomposite. The diffraction rings correspond to the characteristic planes of both CeO_2 and ZnO, indicating the successful formation of a heterostructure that promotes effective charge separation and enhances photocatalytic activity [42]. The lattice fringes observed in high-resolution TEM (HRTEM) images were measured to be approximately 0.26 nm for the (111) plane of CeO_2 and 0.25 nm for the (002) plane of ZnO (data not shown). These measurements suggest a strong interface between the two components, which is essential for the improved photocatalytic performance during the photooxidation of antibiotics [43].

3.8. BET analysis results of of CeO_2 /ZnO Photocatalysts

Figure 8 (a) and (b) show the analysis of the surface area and pore size distribution of the CeO_2-ZnO nanocomposite via the BET N_2 adsorption–desorption isotherm method. The N_2 adsorption–desorption isotherms of ZnO-CeO_2 display a H4-type hysteresis loop and show a BET specific surface area of 30 m^2g^{-1} and a pore diameter of 3.3 nm [44].

Figure 8. (a) N2 adsorption-desorption isoterms and (b) pore size distribution of ZnO/ CeO2 nanocomposite

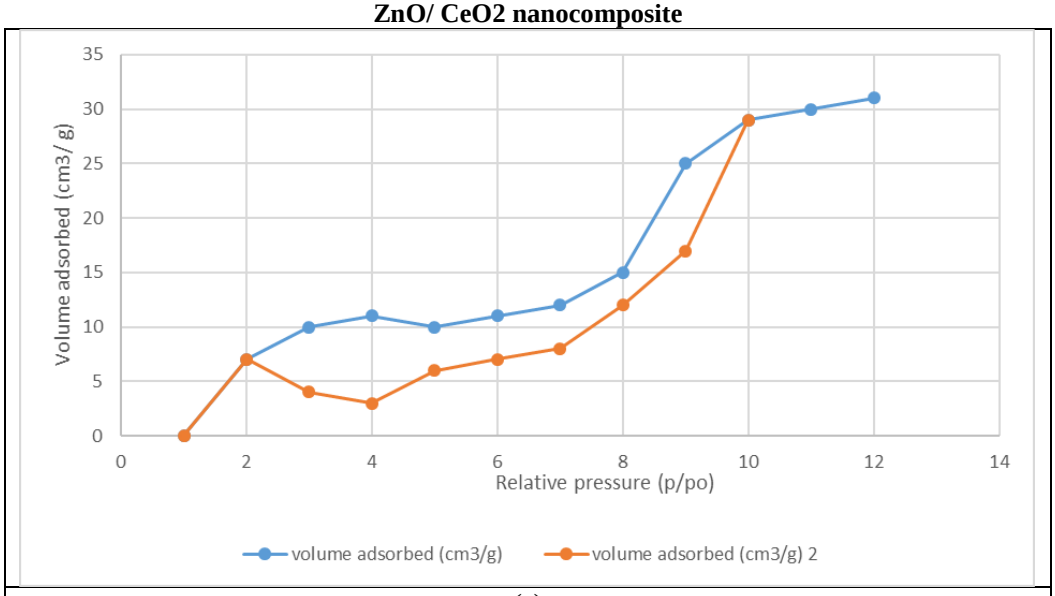

(a)

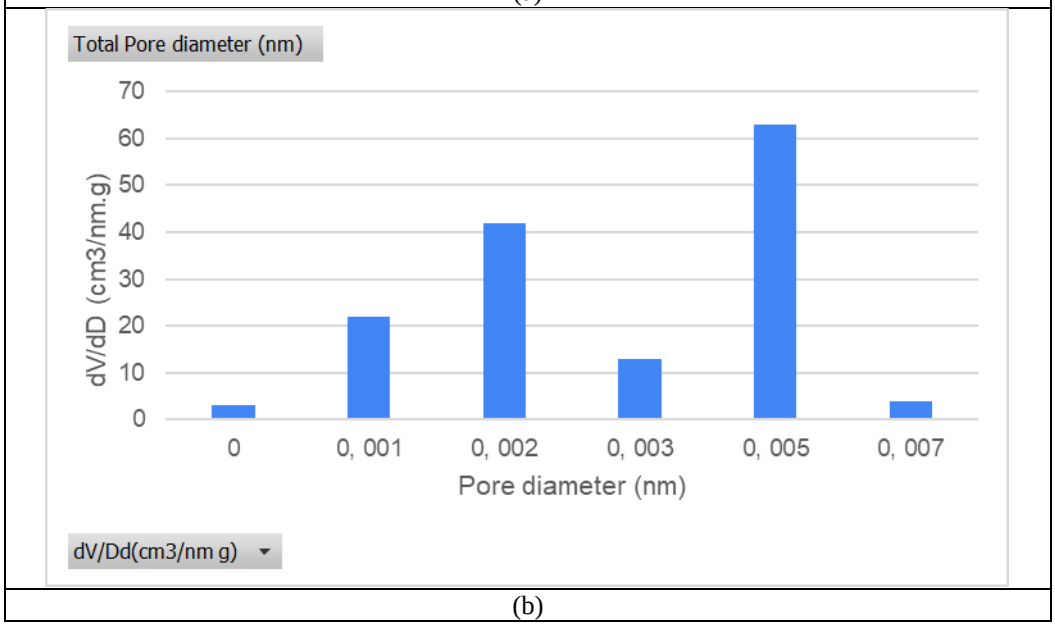

(b)

3.2. Photocatalytic degradation of roxithromycin and Erythromycin antibiotics

Table 1 shows the degradation percentage of 500 mg/l roxithromycin and erythromycin antibiotics versus 45 W/m^2 sunligth irradiation time in the presence of 5 mg/l CeO_2-ZnO nanocomposite. 98% and 96% roxithromycin and erythromycin was detected, respectively, after 30 min photodegradation time. Further increase of time did not affect the photodegradation yields of both antibiotics. As it would be expected, the photodegradation efficiency of both antibiotic increases with an increased exposure time up to a maximum level [44]. The illumination duration should be kept at low levels when studying the photodegradation to avoid inappropriately relating the exposure doses of organics.

Table 1. Photodegradation yields of roxithromycin and erythromycin antibiotics versus irradiation time

	Photoremoval yields (%)			
	Photodegradation time (min)			
Antibiotics	10	20	30	40
Roxithromycin	65	80	98	98
Erythromycin	60	79	96	96

Catalyst loading is another factor that has been shown to affect the efficiency of the photodegradation. As it would be expected, an increase in the amount of catalyst leads to higher photodegradation efficiencies and increased reaction rates as more active sites are provided for adsorption of antibiotic molecules. In fact, the initial reaction rates were found to increase proportionally with the amount of the catalyst. İn this study the maximum photodegradation of roxithromycin (98%) and erythromycin (96%) antibiotics was detected at 5 mg/l CeO_2-ZnO nanocomposite concentration (Table 2). Further increase of nanocomposite dose did not improve the both antibiotic yields. For heterogenic photocatalysis this can be explained by an increase in the suspension's turbidity, which leads to more dominant light scattering phenomena, resulting in limited light absorption by the photocatalyst surface. Moreover, optimum photocatalyst loading depends on the initial solute concentration, therefore, the higher the initial antibiotic concentration, the higher the optimum amount of photocatalyst required for its photodegradation. Thus, an optimum amount of photocatalyst does exist and should be determined first, not only to ensure efficient photodegradation, but also to avoid unnecessary use of catalyst excess [45].

Table 2. Photodegradation yields of roxithromycin and erythromycin antibiotics versus increasing CeO_2-ZnO nanocomposite

	Photoremoval yields (%)			
	CeO_2-ZnO nanocomposite concentration (mg/l)			
Antibiotics	1	3	5	7
Roxithromycin	60	86	98	96
Erythromycin	50	80	96	94

The concentrations of roxithromycin and erythromycin antibiotics strongly influenced the photodegradation yields of these antibiotics. Antibiotic concentration is closely related to aggregation. The higher the antibiotic concentration, the greater the average size of the antibiotic aggregates, thus, the lower the relative surface area accessible to environmental factors that lead to low antibiotic yields. Therefore, an increase in antibiotic concentration leads to an increase in aggregation, resulting in slower photofading rates. Apart from an increase in aggregation, increased antibiotic concentrations may also lead to higher absorption on the surface and weaker interactions between the substrate and the antibiotic, resulting again in lower reaction rates. In this study the maximum roxithromycin (98%) and erythromycin (96%) antibiotic yields was detected up to a 700 mg/l antibiotic concentration. In this study the limit for antibiotic concentration was found to be 600 mg/l (Table 3). In heterogeneous photocatalytic systems the initial antibiotic concentration is shown to have a strong influence on the photodegradation mechanism. It was found that an increase in the antibiotic concentration leads to reduced photodegradation efficiencies and lower reaction rates [46].

Table 3. Photodegradation yields of roxithromycin and erythromycin antibiotics versus increasing antibiotic concentrations

	Photoremoval yields (%)			
	Antibiotic concentration (mg/l)			
Antibiotics	300	400	600	700
Roxithromycin	98	98	98	76
Erythromycin	96	96	96	72

pH in wastewater may be significantly influence the antibiotic yields. Redox active groups can be protonated or deprotonated in acidic or alkaline pH, respectively. The effects of the pH are different for antibiotics depending on their chemical structure and pKa value. In general, charged molecules are more prone to initiate a photodegradation reaction. Therefore, the photodegradation of acidic antibiotics has been shown to increase at pH values higher than their pKa, where these molecules are mostly negatively charged. In this study the maximum roxithromycin and erythromycin antibiotic yields was detected at a pH of 8.00 (Table 4). It is also worth noting that changes in the pH leading to protonation or deprotonation may induce alterations in the conjugated system of the antibiotics, thereby changing their absorption spectrum which should be taken into account when performing light-induced degradation studies in solution. In heterogeneous photocatalytic systems, photodegradation is indirectly influenced by the solution pH, depending on both the catalyst and the dissolved dye. In particular, pH affects the electrostatic interactions between the molecules on the antibiotic molecules, thus, the adsorption capacity of the catalyst is altered. Therefore, at a lower pH protonation of the photocatalyst will take place, leading to a positively charged surface, whereas at higher pH values a negatively charged surface will be formed [47-49].

Table 4. Photodegradation yields of roxithromycin and erythromycin antibiotics versus increasing antibiotic concentrations

	Photoremoval yields (%)			
	pH			
Antibiotics	4	7	8	9
Roxithromycin	45	78	98	66
Erythromycin	40	76	96	70

3.3. Kinetic analysis

The kinetics of photooxidation for roxithromycin and erythromycin in antibiotic-containing wastewater were examined using the CeO_2 /ZnO nanocomposite as a catalyst. The reaction rates were analyzed through pseudo-first-order kinetics, which is commonly applied in the photodegradation of antibiotics. The rate constants (k) for the photooxidation reactions were calculated from the linear plots of $\ln(C_0 /C)$ versus time (t), where C_0 is the initial concentration and C is the concentration at time t. The photodegradation of 500 mg/l roxithromycin and erythromycin antibiotics followed pseudo-first order kinetics (Figure 9). The corresponding apparent first order kinetic rate constant for the photocatalysis of roxithromycin and erythromycin ROX were found as 0.0184 h^{-1} and 0.0073 h^{-1}, respectively.

Figure 9. Pseudo-first-order photodegradatipn kinetics of 500 mg/l roxithromycin and erythromycin antibiotics at 5 mg/l CeO_2 /ZnO nanocomposite after 30 min

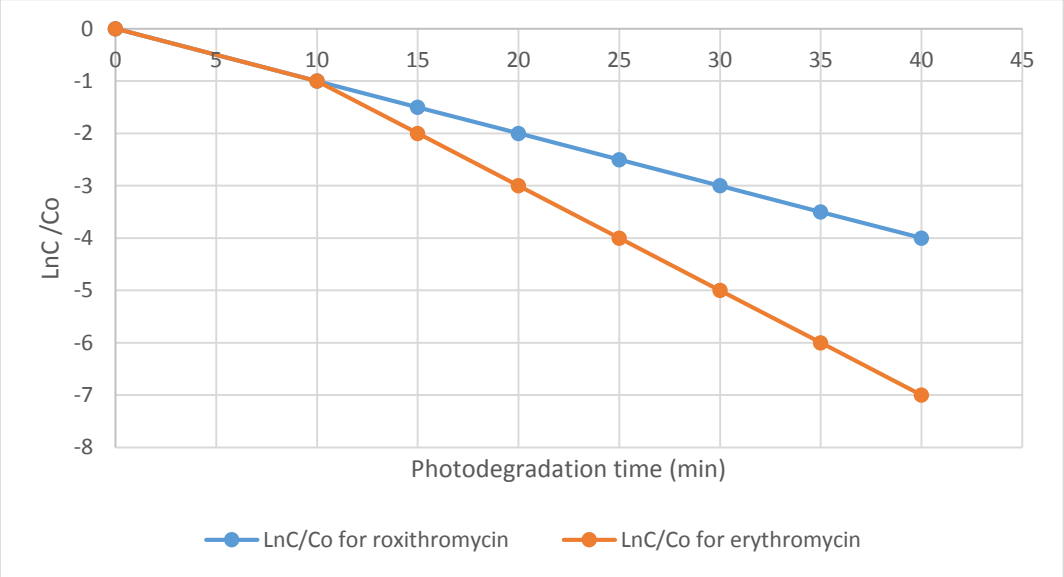

IV. CONCLUSIONS

This study investigated the photooxidation of roxithromycin and erythromycin from antibiotic-containing wastewater utilizing a CeO_2 /ZnO nanocomposite as a photocatalyst. The results demonstrated that the CeO_2 /ZnO nanocomposite exhibited significant photocatalytic activity under sun ligth irradiation, effectively facilitating the degradation of both antibiotics. Kinetic analysis revealed that the degradation process followed pseudo first-order kinetics.

The optimal parameters for the photocatalytic process were identified, including catalyst dosage, initial antibiotic concentration, and pH, which significantly influenced the photodegradation efficiency. The findings underscore the potential of utilizing nanocomposite materials for wastewater treatment applications, particularly in the removal of persistent pharmaceutical and antibiotic contaminants.

Further research is recommended to explore the long-term stability of the CeO_2 /ZnO nanocomposite, as well as the mechanism underlying the photocatalytic degradation process. Additionally, field studies should be conducted to assess the applicability of this technology in real wastewater treatment scenarios.

REFERENCES

[1]. S. Babić, L. Ćurković, D. Ljubas, M. Čizmić TiO2 assisted photocatalytic degradation of macrolide antibioticsCurr. Opin. Green Sus. Chem., 6 (2017), pp. 34-41

[2]. S. Bahnmüller, U.v Gunten, S. Canonica Sunlight-induced transformation of sulfadiazine and sulfamethoxazole in surface waters and wastewater effluents Water Res., 57 (2014), pp. 183-192

[3]. S.R. Batchu, V.R. Panditi, K.E. O'Shea, P.R. Gardinali Photodegradation of antibiotics under simulated solar radiation: implications for their environmental fate Sci. Total Environ., 470–471 (2014), pp. 299-310

[4]. A.P.S. Batista, A.C.S.C. Teixeira, W.J. Cooper, B.A. Cottrell Correlating the chemical and spectroscopic characteristics of natural organic matter with the photodegradation of sulfamerazine Water Res., 93 (2016), pp. 20-29 [

[5]. Baumann, K. Weiss, D. Maletzki, W. Schüssler, D. Schudoma, W. Kopf, U. Kühnen Aquatic toxicity of the macrolide antibiotic clarithromycin and its metabolites Chemosphere, 120 (2015), pp. 192-198

[6]. P. Calza, S. Marchisio, C. Medana, C. Baiocchi Fate of antibacterial spiramycin in river waters Anal. Bioanal. Chem., 396 (2010), pp. 1539-1550

[7]. K.M. Cawley, Julie A. Korak, F.L. Rosario-Ortiz Quantum yields for the formation of reactive intermediates from dissolved organic matter samples from the Suwannee River Environ. Eng. Sci., 32 (1) (2015), pp. 31-37

[8]. K. Choi, Y. Kim, J. Jung, M.H. Kim, C.S. Kim, N.H. Kim, J. Park Occurrences and ecological risks of roxithromycin, thimethoprim, and chloramphenicol in the Han River, Korea Environ. Toxicol. Chem., 27 (3) (2008), pp. 711-719

[9]. D. Fatta-Kassinos, M.I. Vasquez, K. Kummerer Transformation products of pharmaceuticals in surface waters and wastewater formed during photolysis and advanced oxidation processes - degradation, elucidation of byproducts and assessment of their biological potency Chemosphere (2011), pp. 693-709

[10]. M. Herrmann, J. Menz, O. Olsson, K. Kummerer Identification of phototransformation products of the antiepileptic drug gabapentin: biodegradability and initial assessment of toxicity Water Res., 85 (2015), pp. 11-21.

[11]. M. Isidori, Margherita Lavorgna, A. Nardelli, L. Pascarella, A. Parrella Toxic and genetoxic evaluation of six antibiotics on non-target organisms Sci. Total Environ., 346 (2005), pp. 87-98

[12]. H.Y. Kim, S.H. Yu, M.J. Lee, T.H. Kim, S.D. Kim Radiolysis of selected antibiotics and their toxic effects on various aquatic organisms Radiat. Phys. Chem., 78 (2009), pp. 267-272

[13]. Kwiecień, J. Krzek, P. Żmudzki, U. Matoga, M. Długosz, K. Szczubiałka, M. Nowakowska Roxithromycin degradation by acidic hydrolysis and photocatalysis Anal. Methods, 6 (2014), pp. 6414- 6423

[14]. Albrich WC, Monnet DL, Harbarth S. Antibiotic selection pressure and resistance in Streptococcus pneumoniae and Streptococcus pyogenes. Emerg Infect Dis 2004;10: 514–7. 15.An T, Yang H, Li G, Song Cooper WJ, Nie X. Kinetics and mechanism of advanced oxidation processes (AOPs) in degradation of

[15]. An T, Yang H, Li G, Song W, Cooper WJ, Nie X. Kinetics and mechanism of advanced oxidation processes (AOPs) in degradation of ciprofloxacin in water. Appl Catal B- Environ 2010;94:288–94.

[16]. Andersen SR, Sandaa RA. Distribution of tetracycline resistance determinants among gram-negative bacteria isolated from polluted and unpolluted marine-sediments. Appl Environ Microbiol 1994;60:908–12.

[17]. Avisar D, Lester Y, Mamane H. pH induced polychromatic UV treatment for the removal of a mixture of SMX, OTC and CIP from water. J Hazard Mater 2010;175:1068–74.

[18]. Baeza C, Knappe DRU. Transformation kinetics of biochemically active compounds in low-pressure UV photolysis and UV/H2O2 advanced oxidation processes. Water Res 2011;45:4531–43.

[19]. Batchu SR, Quinete N, Panditi VR, Gardinali PR. Online solid phase extraction liquid chromatography tandem mass spectrometry (SPE-LC–MS/MS) method for the determination of sucralose in reclaimed and drinking waters and its photo degradation in natural waters from South Florida. Chem Cent J 2013;7:141.

[20]. Batt AL, Aga DS. Simultaneous analysis of multiple classes of antibiotics by ion trap LC/MS/MS for assessing surface water and groundwater contamination. Anal Chem 2005:77.

[21]. Belden JB, Maul JD, Lydy MJ. Partitioning and photo degradation of ciprofloxacin in aqueous systems in the presence of organic matter. Chemosphere 2007;66:1390–5.

[22]. Bonvin F, Omlin J, Rutler R, Schweizer WB, Alaimo PJ, Strathmann TJ, et al. Direct photolysis of human metabolites of the antibiotic sulfamethoxazole: evidence for abiotic back-transformation. Environ Sci Technol 2013;47:6746–55.

[23]. Boreen AL, Arnold WA, McNeill K. Photochemical fate of sulfa drugs in the aquatic environment: sulfa drugs containing five-membered heterocyclic groups. Environ Sci Technol 2004;38:3933–40.

[24]. Boreen AL, Arnold WA, McNeill K. Triplet-sensitized photodegradation of sulfa drugs containing six-membered heterocyclic groups: identification of an SO2 extrusion photoproduct. Environ Sci Technol 2005;39:3630–8.

[25]. Brown KD, Kulis J, Thomson B, Chapman TH, Mawhinney DB. Occurrence of antibiotics in hospital, residential, and dairy, effluent, municipal wastewater, and the Rio Grande in New Mexico. Sci Total Environ 2006;366:772–83.

[26]. Burns JM, Cooper WJ, Ferry JL, King DW, DiMento BP, McNeill K, et al. Methods for reactive oxygen species (ROS) detection in aqueous environments. Aquat Sci 2012;74:683–734.

[27]. Cals JWL, Hopstaken RM, Le Douxa PHA, Driessen GA, Nelemans PJ, Dinant GJ. Dose timing and patient compliance with two antibiotic treatment regimens for lower respiratory tract infections in primary care. Int J Antimicrob Agents 2008;31:531–6.

[28]. Chamberlain E, Adams C. Oxidation of sulfonamides, macrolides, and carbadox with free chlorine and monochloramine. Water Res 2006;40:2517–26.

[29]. Chee-Sanford JC, Aminov RI, Krapac IJ, Garrigues-Jeanjean N, Mackie RI. Occurrence and diversity of tetracycline resistance genes in lagoons and groundwater underlying two swine production facilities. Appl Environ Microbiol 2001;67:1494–502.

[30]. Costanzo SD, Murby J, Bates J. Ecosystem response to antibiotics entering the aquatic environment. Mar Pollut Bull 2005;51:218–23. Crosby NT. Determination of veterinary residues in food. England: Woodhead Publishing Limited, Abington, Cambridge, 1991.

[31]. Dodd MC, Kohler HPE, Von Gunten U. Oxidation of antibacterial compounds by ozone and hydroxyl radical: elimination of biological activity during aqueous ozonation processes. Environ Sci Technol 2009;43:2498–504.

[32]. Gartiser S, Urich E, Alexy R, Kummerer K. Ultimate biodegradation and elimination of antibiotics in inherent tests. Chemosphere 2007;67:604–13.

[33]. Ge LK, Chen JW, Wei XX, Zhang SY, Qiao XL, Cai XY, et al. Aquatic photochemistry of fluoroquinolone antibiotics: kinetics, pathways, and multivariate effects of main water constituents. Environ Sci Technol 2010;44:2400–5.

[34]. Giger W, Alder AC, Golet EM, Kohler HPE, McArdell CS, Molnar E, et al. Occurrence and fate of antibiotics as trace contaminants in wastewaters, sewage sludges, and surface waters. Chimia 2003;57:485–91.

[35]. Golet EM, Alder AC, Hartmann A, Ternes TA, Giger W. Trace determination of fluoroquinolone antibacterial agents in solid-phase extraction urban wastewater by and liquid chromatography with fluorescence detection. Anal Chem 2001;73:3632–8.

[36]. Isidori M, Lavorgna M, Nardelli A, Pascarella L, Parrella A. Toxic and genotoxic evaluation of six antibiotics on non-target organisms. Sci Total Environ 2005;346:87–98.

[37]. Ravishankar, T.N.; Nagaraju, G. Synthesis and characterization of CeO2 nanoparticles via solution combustion method for photocatalytic and antibacterial activity studies. Chemistry 2015, 4, 146–154. [CrossRef] [PubMed]

[38]. Mishra, P.K.; Vaidya, B. Zinc oxide nanoparticles: A promising nanomaterial for biomedical applications. Drug Discov. Today 2017, 22, 1825–1834. [CrossRef]

[39]. Davis, K.; White, J. Band gap engineered zinc oxide nanostructures via a sol–gel synthesis of solvent driven shape-controlled crystal growth. RSC Adv. 2019, 9, 14638–14648. [CrossRef]
[40]. Wang, Z.L. Zinc oxide nanostructures: Growth, properties and applications. J. Phys. Condens. Matter 2004, 16, R829–R858. [CrossRef]
[41]. Zhong, Q.; Matijevic, E. Preparation of uniform zinc oxide colloids by controlled double-jet precipitation. J. Mater. Chem. 1996, 6, 443–447. [CrossRef]
[42]. Wang, L.; Muhammed, M. Synthesis of zinc oxide nanoparticles with controlled morphology. J. Mater. Chem. 1999, 9, 2871–2878. [CrossRef]
[43]. Bahnemann, B.W.; Hoffmann, M.R. Preparation and characterization of quantum size zinc oxide: A detailed spectroscopic study. J. Phys. Chem. 1987, 91, 3789–3798. [CrossRef]
[44]. Zhang, H.; Que, D. Synthesis of flower-like ZnO nanostructures by an organic-free hydrothermal process. Nanotechnology 2004, 15, 622–626. [CrossRef]
[45]. Zhang, J.; Yan, C. Control of ZnO morphology via a simple solution route. Chem. Mater. 2002, 14, 4172–4177. [CrossRef]
[46]. Li, W.J.; Shi, E.W. Hydrothermal preparation of nanometer ZnO powders. J. Mater. Sci. Lett. 2001, 20, 1381–1383. [CrossRef]
[47]. Ramasami, A.K.; Nagabhushana, H.; Nagaraju, G. Tapioca starch: An efficient fuel in the gel-combustion synthesis of photocatalytically and anti-microbially active ZnO nanoparticles. Mater. Charact. 2015, 99, 266–276. [CrossRef]
[48]. Kumar, C.R.; Betageri, V.S.; Nagaraju, G.; Pujar, G.H.; Onkarappa, H.S.; Latha, M.S. Synthesis of core/Shell ZnO/Ag nanoparticles using calotropis gigantea and their applications in photocatalytic and antibacterial Studies. J. Inorg. Organomet. Polym. Mater. 2020, in press. [CrossRef]
[49]. Malleshappa, J.; Vidya, Y.S. Leucasaspera mediated multifunctional CeO2 nanoparticles: Structural, photoluminescent, photocatalytic and antibacterial properties. Spectrochim. Acta Part. A Mol. Biomol. Spectrosc. 2015, 149, 452–462. [CrossRef]